PNAS SPECIAL FEATURE | PSYCHOLOGICAL AND COGNITIVE SCIENCES NEUROSCIENCE

Hippocampal gamma and sharp wave/ripples mediate bidirectional interactions with cortical networks during sleep

Rafael Pedrosa[a,1], Mojtaba Nazari[b], Majid H. Mohajerani[b], Thomas Knöpfel[c], Federico Stella[a,1,2], and Francesco P. Battaglia[a,1,2]

Edited by Lynn Nadel, The University of Arizona, Tucson, AZ; received March 28, 2022; accepted August 12, 2022

Hippocampus–neocortex interactions during sleep are critical for memory processes: Hippocampally initiated replay contributes to memory consolidation in the neocortex and hippocampal sharp wave/ripples modulate cortical activity. Yet, the spatial and temporal patterns of this interaction are unknown. With voltage imaging, electrocorticography, and laminarly resolved hippocampal potentials, we characterized cortico-hippocampal signaling during anesthesia and nonrapid eye movement sleep. We observed neocortical activation transients, with statistics suggesting a quasi-critical regime, may be helpful for communication across remote brain areas. From activity transients, we identified, in a data-driven fashion, three functional networks. A network overlapping with the default mode network and centered on retrosplenial cortex was the most associated with hippocampal activity. Hippocampal slow gamma rhythms were strongly associated to neocortical transients, even more than ripples. In fact, neocortical activity predicted hippocampal slow gamma and followed ripples, suggesting that consolidation processes rely on bidirectional signaling between hippocampus and neocortex.

hippocampus | memory consolidation | cortical networks | gamma oscillations | default mode network

Spontaneous activity during quiescent periods and sleep is likely to be crucial for a multitude of cognitive functions. Functional connectivity studies from human neuroimaging and other brain monitoring modalities have identified several "resting-state networks" whose activity fluctuations are coordinated. One of them, the default mode network (DMN), increases its activity when the brain does not actively drive overt behavior and is involved in functions such as imagery, planning, self-reflection, and memory mechanism (1, 2). The dynamical interplay between hippocampus and the neocortex is another hallmark of the spontaneous activity during behavioral idleness. Hippocampal sharp waves/ripples (SWRs) (3), bursts of hippocampal activity, have attracted most attention as a conduit for this interplay, as they modulate neocortical activity (4–6). Interestingly, the DMN areas are among those most strongly activated at SWR times (7). SWRs are also linked to the bulk of memory replay in the hippocampus, which is the spontaneous repetition of neural activity patterns that were initially elicited during experience (8, 9). Replay has been observed also in many cortical areas (see, e.g., refs. 10–13), most strongly in correspondence with hippocampal SWRs.

The interaction between the hippocampus and the neocortex figures prominently in most theories of explicit memory: The hippocampus is seen as rapidly forming rapid memories and "index codes" that summarize and point to activity patterns (14) that simultaneously (albeit more slowly) form in the neocortex and elsewhere in the brain. At memory retrieval, and during offline periods, those codes would propagate to the neocortex. Here, they would help seamlessly updating a large memory repository, as postulated by the complementary learning systems theory (15), or would create new, multiple memory traces [MMT theory (16)] with either similar content or semantic, gist-like representations (17).

According to all of these theoretical accounts, however, cortico-hippocampal interplay likely involves the entirety of the neocortex. Yet, previous work has concentrated mostly on single neocortical areas, chosen among those with strongest anatomical links to the hippocampus. Functional magnetic resonance imaging (fMRI) (5) and voltage-sensitive imaging data (18) highlight the global character of neocortical activity modulations related to SWR, with a prominent role of the DMN (7), but how information propagates in neocortical networks is not known yet.

During sleep cortical networks are capable of self-sustained high activity transients (UP states, periods of neuronal activation) delimited by silent periods (DOWN states, periods of neuronal silence) (19), generated by recurrent excitation across cortical neurons (20, 21). UP/DOWN state fluctuations have often been described as traveling waves (22–25), but little is known about the structure of each transient activation. Here, with voltage imaging in neocortex of mice combined with layer-resolved

Significance

During sleep, brain is bustling with activity: Different brain structures such as the hippocampus and the cortex interact, and this interplay is thought to be important to stabilize and reprocess memories, in the so-called systems consolidation. We show that during nonrapid eye movement sleep, cortical activity organizes in transient bursts of widely varying size, with a dynamic that may help remote areas communicate with one another. With a data-driven analysis of activity transients we identified three functional networks, one of which, namely the default mode network, most actively interacts with the hippocampus. This interaction is bidirectional and involves multiple patterns of hippocampal activity. We speculate that this information exchange loop subserves complex computational operations that are key to memory functionality.

Author contributions: R.P., M.H.M., F.S., and F.P.B. designed research; R.P. and M.N. performed research; T.K. contributed new reagents/analytic tools; R.P., F.S., and F.P.B. analyzed data; and R.P., M.H.M., T.K., F.S., and F.P.B. wrote the paper.

The authors declare no competing interest.

This article is a PNAS Direct Submission.

[1]To whom correspondence may be addressed. Email: rhapedrosa@gmail.com, federico.stella@donders.ru.nl, or f.battaglia@science.ru.nl.

[2]F.S. and F.P.B. contributed equally to this work.

This article contains supporting information online at http://www.pnas.org/lookup/suppl/doi:10.1073/pnas.2204959119/-/DCSupplemental.

Published October 24, 2022.

hippocampal local field potentials (LFPs), we characterize the probability distribution of transient sizes, showing that it approximates a power-law shape, signature of a near-critical state (in which long-range spatial and temporal correlation are maximized, facilitating global brain coordination), thought to maximize information transmission between far apart cortical sites (26, 27). Thus, these dynamics may be an effective support for the formation of neocortical memory traces.

We further delineate the structure of activity transients in a data-driven manner and we find three functional networks centered respectively on the retrosplenial cortex and medial cortical bank of the cortex, on somatosensory cortex, and on lateral cortex. These networks closely match the results of a large anatomical projections dataset (28). Crucially, we show that they are differentially involved in hippocampal communication, with a "retrosplenial" network, overlapping with the standard DMN playing a prominent role.

All the theoretical accounts mentioned above emphasize the hippocampal influence on the neocortex and a unidirectional flow from the hippocampus to neocortex, embodied in SWRs. Our data from voltage imaging and LFPs from hippocampal subfield CA1 suggest two refinements of this picture. First, the strongest correlate of cortical activity transients is the slow gamma rhythm (20 to 50 Hz), even outpacing SWRs. Slow gamma has been linked with the routing of information from hippocampal subfields CA3 to CA1. The CA3 subfield is rich in recurrent connections, features of an auto-associative memory (29–31). During sleep, increased slow gamma during SWR events correlates with greater replay (32). Furthermore, using pseudocausality analysis we show here that cortical transients in the DMN/retrosplenial network precede bouts of hippocampal slow gamma.

Together, these data point toward a bidirectional interaction as a constituent of the overall architecture of cortico-hippocampal interactions, which provides a potential dynamical scenario. This picture opens up a theoretical view explaining the involvement of the DMN in memory and the two-way exchanges between hippocampus and neocortex, regions crucial for memory and cognition.

Results

Parallel Recordings of Neural Activity Transients in the Cortex and the Hippocampus. We imaged the neocortical spatiotemporal activity in the right hemisphere (24, 33–35) under urethane anesthesia and natural sleep (Fig. 1 *A* and *B* and *SI Appendix*, Fig. S1). For this, we used wide-field macroscopy and a voltage-sensitive dye (VSD) in wild-type C57/Bl6 mice (18, 25, 36) (for the anesthesia experiments) and mice expressing a ratiometric genetically encoded voltage indicator [GEVI; chiVSFP (33, 37–39); for natural sleep, here referred to as VSI]. In both cases, the neocortical voltage activity was simultaneously recorded with the ipsilateral hippocampal LFP (an electrode was placed in dorsal CA1 for the urethane anesthesia recordings and a 16-channel high-density silicon probe recorded signals from all CA1 layers for natural sleep recordings). In the urethane anesthesia experiments, we also sampled cortical electrical activity by use of an electrocorticography (ECoG) 6 × 5 grid placed on the same cortical surface we were imaging.

In neocortex, we observed temporal activity fluctuations spanning a large range of temporal and spatial scales (Fig. 1*C*). We then applied an activity transient detection algorithm based on local and global average neocortical activity (Fig. 1 *D* and *E*; see *SI Appendix*, *Cortical Transient Detection*). Such a method allowed us to isolate temporal windows of excitation spanning variable neocortical extents and to separately analyze the global properties of these activation bouts, such as their duration and size.

Cortical Transients in the Mouse Cortex Show Power-Law-Like Distributions of Size in Anesthesia and Natural Sleep. To characterize the properties of neocortical activity transients, we computed the statistical distribution of transient descriptors such as the overall, cumulative activation of cortex over the duration of the transient (Fig. 2*A* and *SI Appendix*, Fig. S2). In both urethane anesthesia and natural sleep groups we find that the frequency distribution of magnitude-related properties (size and duration) of transients are well-captured by a power law. We nevertheless observe a substantial difference in the goodness of fit between urethane anesthesia and natural sleep recordings: Power-law fits were generally better for sleep data, mostly because anesthesia was associated with a pronounced overabundance of large-sized events (and similarly of longer events), making the overall distribution resemble a supercritical one (40) (urethane anesthesia/VSD group: $\alpha = -1.8775$ and $\varepsilon = 0.2325$ and natural sleep/VSI group: $\alpha = -1.7385$ and $\varepsilon = 0.0856$). Interestingly, such supercriticality is not observed in ECoG recording of the same cortical states (urethane anesthesia/ECoG group: $\alpha = -2.168$ and $\varepsilon = 0.1751$ and urethane anesthesia/ECoG in VSD group: $\alpha = -1.8456$ and $\varepsilon = 0.2106$), suggesting a substantial difference in the signal represented in the two recordings methods. Based on theoretical arguments (41) this may be due to the nonindependence of electrode in the ECoG matrix, because of volume conductance effects. Although different in their statistical properties, VSD and ECoG signals were still strongly correlated, consistently with their being two measures of the same underlying phenomenon (*SI Appendix*, Fig. S2 *B–E*; size correlations: mouse 1 = 0.65, mouse 2 = 0.61, mouse 3 = 0.54, mouse 4 = 0.42 and mouse 5 = 0.5).

A Few Cortical Networks Account for Small Cortical Transients. While size distributions provide information on the relative abundance of smaller vs. larger, global transients, they are not informative about the spatial organization of their events or whether different types of transients exist that span different cortical regions.

To address these questions, we first segmented the neocortical transients in six equal quantiles based on their size (Fig. 2*B*). Then, we classified the spatial patterns of activity by training a restricted Boltzmann machine (RBM) on temporal frames belonging to each of these transient quantiles. The RBM encodes these images based on the statistics of pixels coactivations and the state of each hidden unit state becomes selective for a different recurring arrangement of active pixels. To ascertain whether transient events can be classified in a finite number of discrete categories, we applied a clustering algorithm on the set of learned RBM weights (42) relative to all events (Fig. 2*C* and *SI Appendix*, Fig. S3*F*). We find a marked dependency on the transient size. In both urethane anesthesia and natural sleep groups, transients at the lowest end of the quantile distribution can in fact be neatly subdivided in a very low number of well-separated modes (scatter plots in Fig. 2*C*; EM model fitting resulted in three modes as being the most likely subdivision for four out of five animals for the urethane anesthesia group and four out of five animals for the natural sleep group. The cluster separation was confirmed by the strong bimodal distribution of pairwise distances between RBM weight vectors as shown in the histograms). For larger transients, no clearly distinct modes appeared.

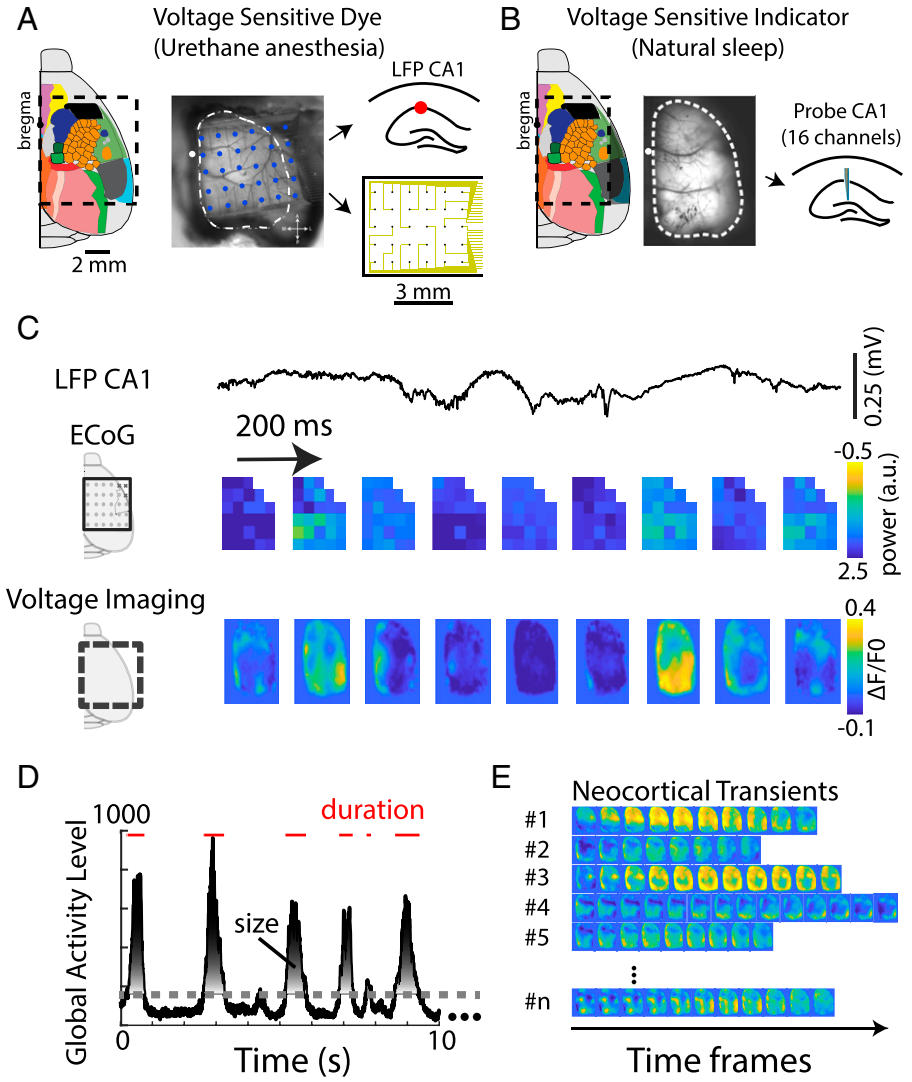

Fig. 1. Experimental setups used for the neocortical transients recording. (*A*) Schematic of wide-field topography (*Left*) and photo of the preparation (*Center*) of the setup for the neocortical voltage-sensitive dye imaging recorded in combination with hippocampal LFP and ECoG in mice under urethane anesthesia. The black dashed line in the diagram (white dashed line in the photo) represents the borders of the camera field of view. Bregma is represented as a black dot. (*Insets*) The transparent ECoG (6 × 5 channels) covering much of the imaging field of view and the location of hippocampal LFP electrode. (*B*) Schematic and photo of ipsilateral wide-field topography of the neocortical voltage-sensitive indicator imaging recorded in combination with a linear silicon probe (16 channels) in the hippocampus. In this experiment, we recorded natural sleep in GEVI mice. Note that imaged region is smaller than in the anesthesia group (because skull was not removed, but only thinned). (*C*) Example traces of hippocampal LFP, ECoG, and VSD signals (anesthesia group). (*D*) Global activity level of the neocortex recorded by the VSD. The shadowed area represents the size of the transient, defined by the area under the curve, and red lines highlight the intervals relative to each transient. (*E*) Examples of detected neocortical transients.

While large activations consist of the simultaneous activation of large swaths of cortical surface, small ones disproportionally involve a handful of networks centered around, respectively, retrosplenial cortex (RS), temporal association area (TeA), and somato-sensory (SS) (Fig. 2*D*). Further inspection of the spatial organization of the RBM-identified modes reveals a tendency for these areas to form pairwise activation patterns (*SI Appendix*, Fig. S3*G*). Thus, a set of well-defined networks appear to dominate the small activity fluctuations which make for the vast majority of transient cortical activity.

Large Cortical Transients Are Most Often Preceded by RS or SS Activation. As seen from the analysis above, large neocortical transients in both urethane anesthesia and natural sleep could not be straightforwardly classified in a handful of modes. In fact, activity propagation during these periods does not seem to follow stereotypical dynamical patterns (Movie S1). Instead, we actually found that large transients (in particular those in the sixth and largest quantile) mostly differ by the activation patterns immediately preceding them. When applying the same previous RBM-based analysis on time frames extracted from short periods (~100 ms) immediately preceding the detected onset of the large transient, we found activation modes resembling those of Fig. 2*C*, with activations preceding last-quantile transients neatly clustering into a couple of well-separated groups (Expectation Maximization model fitting resulted in two modes as being the most likely subdivision for five out of five animals for the urethane anesthesia group and three out of five animals for the natural sleep group; Fig. 2*E*). This is, however, not the case for smaller transients.

In both urethane anesthesia and natural sleep groups, activity preceding large transients is found to be concentrated either in the medial-posterior portion of the cortex, around the RS, or laterally around the SS. Thus, we can conclude that large transients are triggered by small and focused activity bouts and also that such preactivations are mostly confined to two well-defined

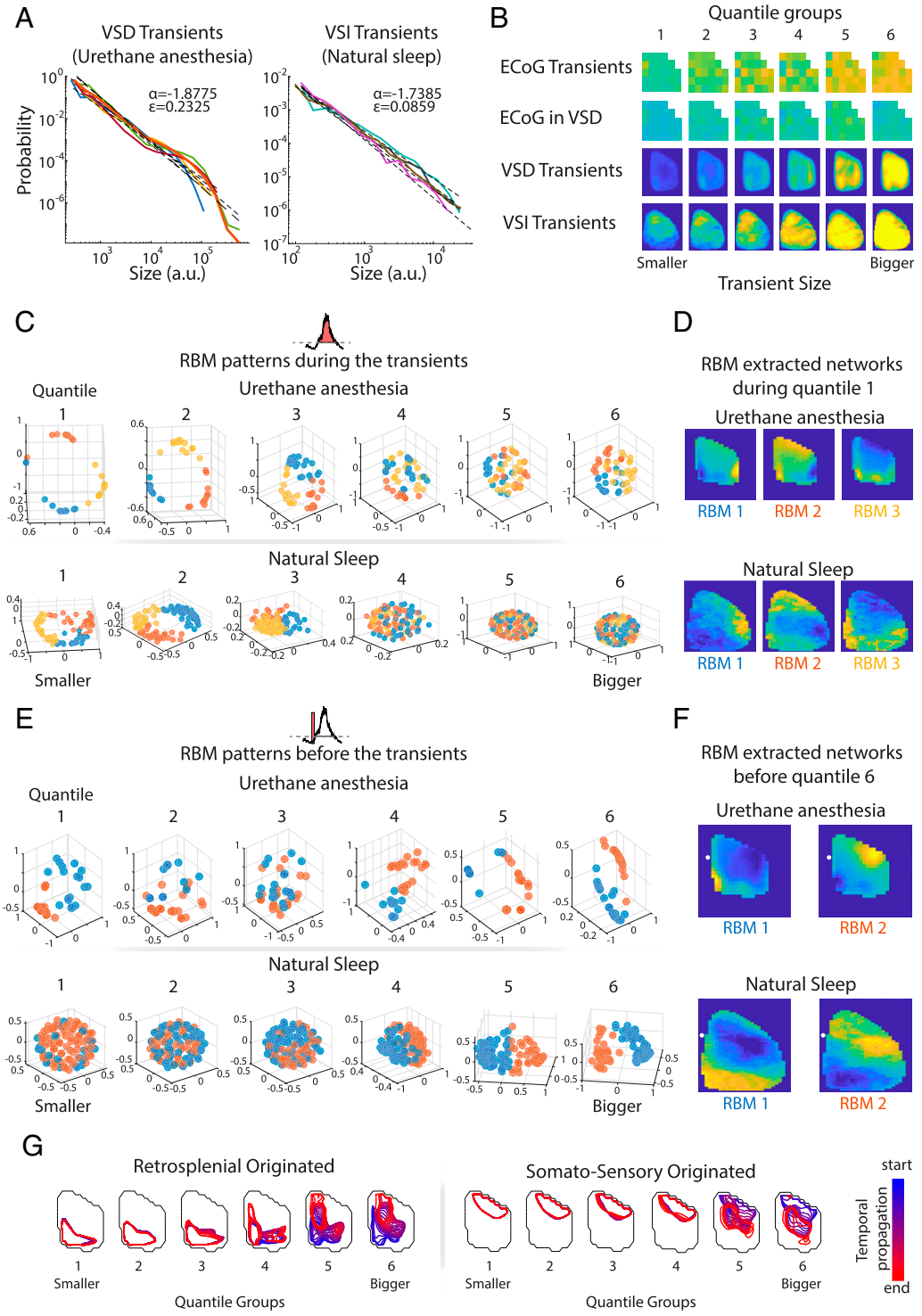

Fig. 2. Probability distribution of transient sizes in urethane anesthesia and natural sleep reveals different modular networks for small neocortical transients. (*A*) Transient probability density size in urethane-anesthetized and natural sleep states. For both urethane and natural sleep datasets, we computed the size of transients detected and measured from the VSD and VSI data. For the natural sleep dataset, we computed neocortical transients of the VSI data during the NREM periods (iv, see *Materials and Methods* for the sleep state detection). Lines of different colors represent different animals. Note that the animals from the natural sleep code have a different color code. The black dashed lines represent the linear regression (in log-log scale) for each animal. α is the critical exponent (slope of the regression line) and ε the fitting error (see *Materials and Methods*). a.u., arbitrary units. (*B*) Neocortical average signals for the transients subdivided in sox quantiles based on the size shown in *A*. (*C*) Example of RBM weights (reduced to three dimensions by principal component analysis) computed on each of the six quantile groups distributed by the transient size for urethane anesthesia and natural sleep data. The blue, orange, and yellow colors denote three clusters separated by using the *k*-means algorithm. Note that for both datasets a tendency for clustering in the RBM weights can be observed in smaller transient groups. (*D*) Spatial distribution of activity corresponding to the three *k*-means clusters in the first quartile RBM weights. (*E*) Example of RBM weights computed from cortical activations 100 ms before the transient onset for each of the six size quantiles for urethane anesthesia and natural sleep data. The blue and orange colors represent two clusters separated by *k*-means for each quantile. The respective yellow histograms show the distributed cosine distance for each individual pretransient. Note that for both datasets a dissociation in the RBM weights can be better observed in the bigger transient groups. (*F*) Spatial distribution of activity corresponding to the two *k*-means clusters in the sixth quartile RBM weights. (*G*) Spatiotemporal evolution of the transients triggered by RS or SS modes. The panel shows the average temporal propagation profile (blue: transient start, red: transient end) for each quantile.

cortical regions (Fig. 2*F*). While smaller events happening to originate in the RS or SS area remained largely confined to the same area for their entire duration, larger events have a growing chance of "spilling over" (Fig. 2*G* and *SI Appendix*, Fig. S4*D*). Both RS-led and SS-led transients of large size are found to involve different cortical networks over their evolution, generally terminating in the central area of the imaged cortical surface, or even invading the opposite network (so RS activation eventually leads to an activation of the SS network, and vice versa) (Movies S2 and S3). These findings highlight the presence of two, largely independent cortical networks, one centered around the RS cortex and the other around the SS region (28).

Neocortical Transients Preferentially Correlate with Slow Gamma Activity in the Hippocampus. We then considered what the functional repercussions of transient activity and its structure can be. In particular, cortical sleep activity has been connected to interactions with the hippocampus, possibly supporting memory consolidation (15).

In order to explore this question, we analyzed the relationship between global cortical transients and hippocampal LFPs. We concentrated on two frequency bands that have been associated to cortico-hippocampal communication, gamma (20 to 80 Hz), involved in entorhinal-hippocampal and prefrontal-hippocampal interactions (29, 30), and ripple (150 to 250 Hz), a component of the SWR complex thought to be a main carrier of hippocampal input to the cortex (4, 6).

By averaging the hippocampal CA1 LFP in coincidence with neocortical transients, separately for events belonging to each of the six size quantiles defined above, we observed different patterns in the distribution of LFP power density with increasing transient size (Fig. 3*A*). The frequency bands of interests, gamma and ripple, appeared to be prominent in the hippocampal LFP spectrum and modulated by the transient size. Indeed, power in both frequency bands showed a significant correlation with simultaneous transient size (Spearman correlation, urethane gamma and ripple $R = 1$, $P = 0.001$, sleep gamma $R = 1$, $P = 0.001$, ripple $R = 0.7$ $P = 0.05$; Fig. 3*B*). The two bands appeared nevertheless to follow different patterns, with gamma power presenting a linear increase with transient size, while ripple power followed a sigmoid-like trend (indeed ripple power correlation in sleep was only marginally significant, $P = 0.05$).

To further characterize interactions between hippocampal gamma and cortical activity, in the natural sleep group we looked at layer-resolved signals from linear silicon probe recordings to distinguish between gamma sources at different depths in CA1. Based on existing literature (43, 44), distinct gamma power was computed from the subsequent source area: slow gamma (20 to 50 Hz, stratum radiatum), medium gamma (60 to 90 Hz, stratum lacnosum moleculare), and high gamma (100 to 140 Hz, stratum pyramidale). We observed that mostly slow gamma showed a modulation with the transient size (*SI Appendix*, Fig. S5*A*). In order to isolate any effect of the volume conduction, we computed gamma power of the current source density (CSD) signal across different transient sizes. Using the CSD signal, we compared slow gamma activity obtained from different hippocampal layers. The result confirmed slow gamma modulation to be stronger in the stratum radiatum (Fig. 3*C*; Spearman correlation, $R = 0.8$ $P = 0.01$).

Thus, hippocampal gamma appears to be associated with global cortical activation to at least a similar extent as SWR, which is considered the hallmark of cortico-hippocampal interactions.

Slow Gamma Accounts for Correlations between SWR and Cortical Activations. As previously reported, SWR events are associated to slow oscillations in the cortex (4), and more recently they have been found to be especially correlated to a network centered around retrosplenial cortex (7, 11, 18, 45). To establish the relevance of SWR events for cortical excitation, we replicated in both urethane anesthesia and natural sleep datasets the approach used by Karimi Abadchi et al. (18). As shown in those studies, we also find that a cooccurrence measure of correlation between SWR events and cortical activation identifies RS as the main hotspot (*SI Appendix*, Fig. S5 *B* and *C*), but which feature of the SWR complex is mainly responsible for such relationship? Indeed, SWRs and slow gamma events appear to be highly correlated in time (32) (Fig. 3*D*), causing their contribution to be potentially intermingled. To answer this question, we considered three SWR properties: ripple power component, slow gamma power component, and sharp wave amplitude. Indeed, we find that while ripple power does not correlate with RS activation, the magnitude of the sharp wave component of SWR events does show a significant correlation with the degree of RS activation (correlations: Ripple/RS *R*: 9.3102e-5 and *P*: 0.7642; sharp wave/RS *R*: 0.0045 and *P*: 0.0375). It is nevertheless the slow gamma contribution to the SWR event that appears to have the strongest relationship with RS activity (correlations: slow gamma/RS *R*: 0.0183 and *P*: 2.3407e-5). Remarkably, sharp wave-to-RS correlation is not significant anymore after controlling for the simultaneous slow gamma power by partial correlation analysis (partialized for slow gamma: ripple/RS *R*: −0.0187 and *P*: 0.5609; sharp wave/RS *R*: 0.0081 and *P*: 0.8017). Conversely, the slow gamma-to-RS correlation remains significant after controlling for the simultaneous sharp wave magnitude (partialized for sharp wave amplitude: slow gamma/RS *R*: −0.1183 and *P*: 0.0002). This set of analyses suggests that at least a portion of the reported dependence of cortical activation on SWR occurrence might be ascribed to the gamma component present in the latter.

Transients Triggered by RS Activation Shape Gamma but Not SWR in the Hippocampus. We then asked how our classification of neocortical transients fits into this emerging picture of cortico-hippocampal interactions. We thus repeated the previous analysis using RS-led and SS-led transients separately. Visualizing the average LFP power for different sets of events already makes evident a stark differentiation between the transient families (Fig. 4*A*). RS-led events appear to elicit a much stronger response in the hippocampus, both under urethane anesthesia and in natural sleep groups. By quantifying this effect, we find it to be specific to the gamma band of the power spectrum (Fig. 4*B* and *SI Appendix*, Fig. S6*B*; two-way ANOVA; urethane anesthesia: gamma+RS/SS: bins 1–4, $P < 0.05$; ripple+RS/SS: not significant; natural sleep: gamma+RS/SS: bins 4, $P < 0.05$; ripple+RS/SS: not significant). Only SS-led transients of major size are found to elicit a comparable gamma activation in the hippocampus. We speculate that this might possibly happen as a consequence of the transient spilling previously described, in which case an initially SS-triggered event would eventually result in a delayed RS activation. On the other hand, ripple power turned out to be largely independent of the transient identity, consistently with our previous analysis of the SWR–RS relationship.

This interaction can be further specified by comparing the magnitude of the RS cortex preactivation with the elicited power in the gamma or ripple band (Fig. 4*C* and *SI Appendix*, Fig. S6*B*). By computing the correlation within groups of events of comparable size we find that RS preactivation scales consistently

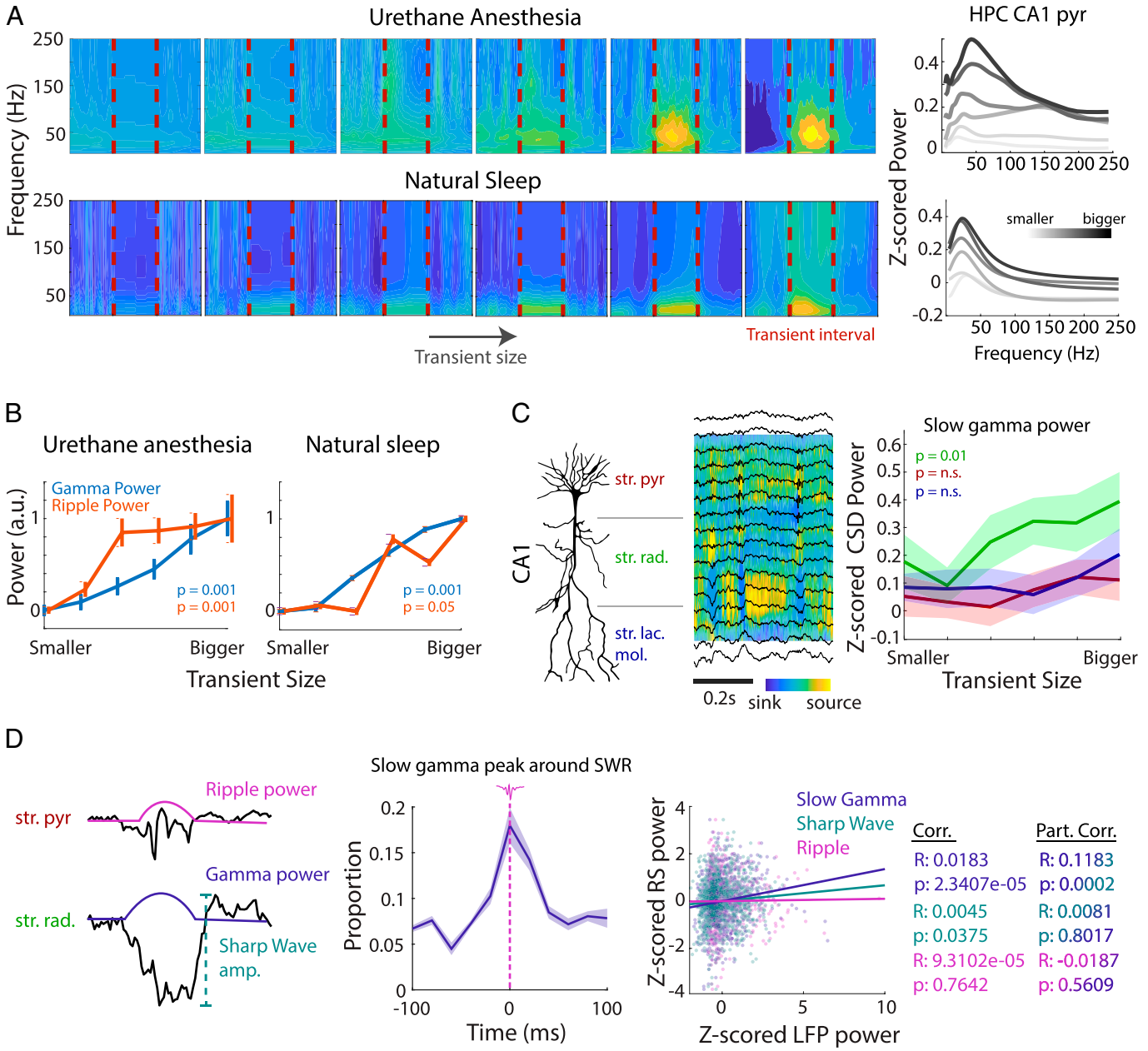

Fig. 3. Neocortical transient's interactions with hippocampal slow gamma and SWR. (*A*) CA1 LFP spectrogram (*Left*) and power spectra (*Right*) during transients in the six quantiles in urethane anesthesia and natural sleep data, averaged across animals. Note that the presence of gamma activity during the transients is proportional to the transient size (a.u. = arbitrary units). (*B*) Averaged gamma (20 to 80 Hz) and ripple (150 to 250 Hz) power normalized between 0 and 1 across animals in different transient sizes. (Spearman's rank correlation coefficient, $n = 5$ animals). (*C*, *Left*) depiction of CA1 layers overlayed on a pyramidal neuron silhouette. (*C*, *Center*) Layer-resolved LFP (traces) and CSD (color image) from the CA1 layers. (*C*, *Right*) Normalized CSD power for slow gamma (20 to 40 Hz) in stratum pyramidale, stratum radiatum, and stratum lacunosum moleculare as a function of transient size during natural sleep. A channel in each CA1 layer was selected to calculate the normalized power. The line and respective shadowed area represent the average across animal and SEM (significance: Spearman one-tailed correlation). (*D*) Interaction between hippocampal LFP and RS activation during SWR. (*Left*) Diagram showing the definition of the three measures (ripple power, sharp wave amplitude and slow gamma power) for which we compute correlations with RS activity. (*Center*) Event-triggered average of slow gamma peaks centered on ripples. (*Right*) Mean normalized RS activity around the SWR (−100 to 100 ms) (*y* axis) against slow gamma, ripple power, and the sharp wave normalized amplitude (*x* axis) in radiatum during the ripples. (*Right*) Correlation of slow gamma-RS partialized for sharp wave amplitude, sharp wave-RS partialized for slow gamma amplitude, and ripple-RS partialized for slow gamma amplitude.

with the degree of gamma engagement, and not the ripple one, during the following cortical transient ($P < 0.05$; two-way ANOVA). This role of RS cortex is time-specific: Using its average activity during the transient, thus during a period of cortical excitation, results in no correlation with hippocampal gamma.

Precise, Bidirectional Temporal Relationships between Cortical and Hippocampal Activations Are Orchestrated by RS. Finally, we investigated the temporal structure of the cortico-hippocampal interactions outlined above. We first computed the cross-correlation between the temporal evolution of hippocampal power in either the ripple or gamma band and the degree of activation of different portions of the cortical surface (Fig. 4*D*). Importantly, we used partial correlations, that is, we computed the correlation between pixel activation and gamma power controlling for ripple power, and vice versa (cortical activity vs. ripple controlling for gamma). Confirming our previous findings, correlations between gamma and cortex are much stronger than those involving ripples. Both in urethane anesthesia and natural sleep recordings correlations appear to follow a precise spatiotemporal pattern.

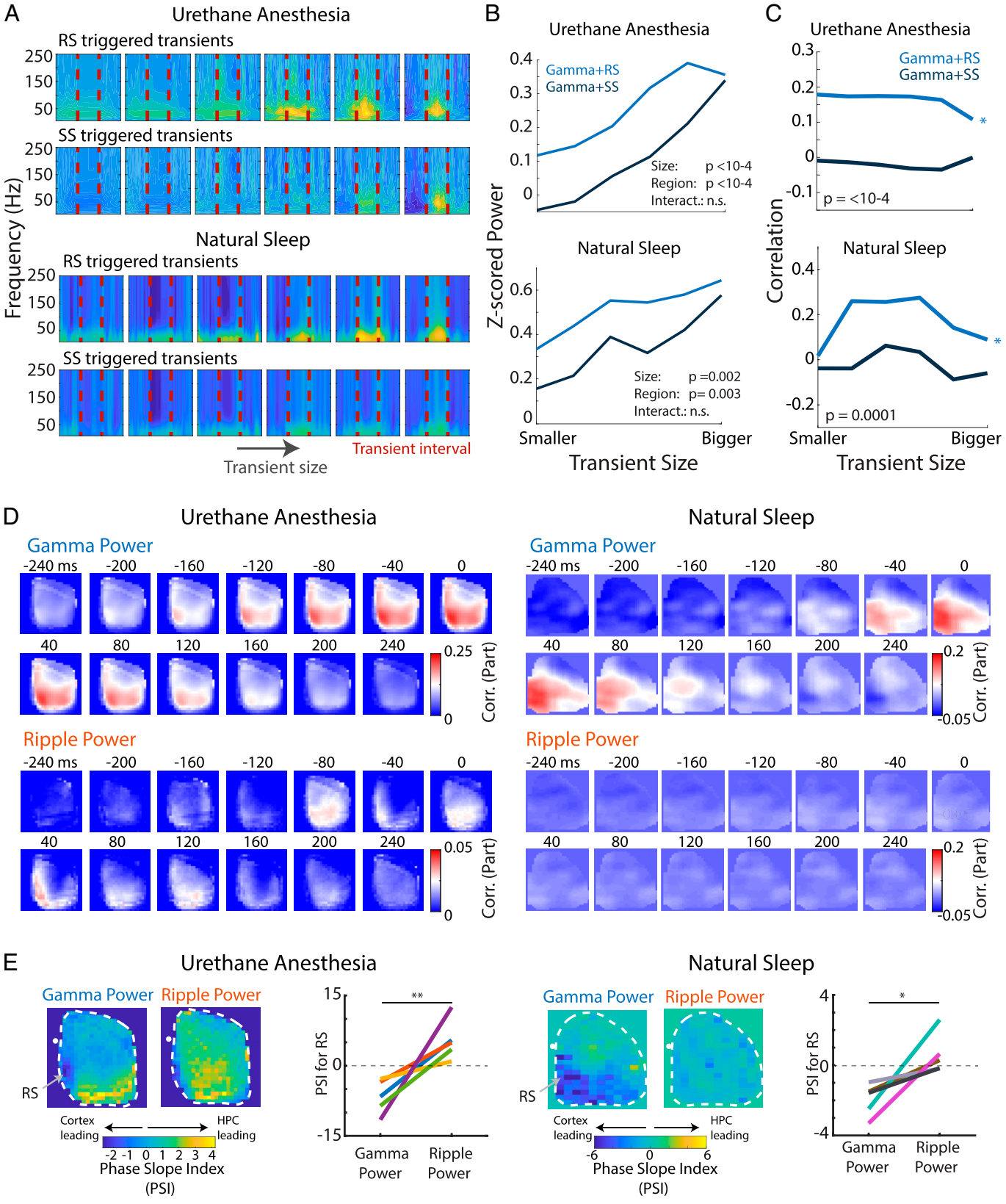

Fig. 4. Neocortical transients triggered by RS influence gamma power in the hippocampus. (*A*) Interpolated CA1 spectrogram during the RS- and SS-triggered transient intervals across different sizes in urethane anesthesia and natural sleep data. (*B*) Normalized power of gamma (20 to 80 Hz) for transients triggered by RS and SS across size (*$P < 0.05$; two-way ANOVA). (*C*) Correlation of gamma with RS- or SS-triggered events within the same block sizes. The panels are the correlation between the hippocampal CA1 LFP and the activity of the period before RS and SS transients. (*D*) Partial correlation between hippocampal gamma power versus the optical temporal signal for each pixel partialized for ripple power and partial correlation between hippocampal ripple power versus the optical temporal signal in each pixel partialized for gamma power. Correlations were calculated from z-scored data. (*E*) Phase slope index for normalized gamma or ripple power versus the optical temporal signal in each pixel. The white dot represents bregma. The gray arrows indicate the position of retrosplenial cortex, which presents a temporal modulation, in gamma but not in ripple, from the cortex to the hippocampus (*$P < 0.05$ and **$P < 0.005$; one-sample *t* test against zero; $n = 5$ animals for the urethane and $n = 5$ for the natural-sleep group represented in different colors).

Positive correlations with gamma power tend to appear at negative time shifts, thus preceding the peak of the gamma power. Also, they are initially localized in areas close to the midline and they mostly involve cortical areas distributed either medially or posteriorly, overlapping with the DMN. In contrast, ripple power is associated with a much weaker coherence in cortical activation and with a higher degree of symmetry around its peak.

Not only then hippocampal engagement is preferentially associated to a network organized around the RS cortex, but such engagement appears to be initiated by the cortex. This view is confirmed when computing the phase slope index (46), a measure of directed causality, between cortical activation at different sites and hippocampal LFP instantaneous power. Conversely, ripple power leads a large swath of the cortex with little spatial specificity. Directionality scores are in fact higher than those obtained from gamma power (Fig. 4*E*). Strikingly, the RS region present an extreme version of this tendency (one-sample *t* test, between gamma and ripple for urethane anesthesia: $P < 0.005$; gamma and ripple for natural sleep: $P < 0.05$; comparing to zero, urethane anesthesia: gamma $P < 0.005$, ripple $P < 0.05$ and natural sleep: gamma $P < 0.005$, Ripple, not significant). Interaction directionality scores computed from this area in fact present an almost complete switch between gamma and ripple power band: they are consistently negative in the former case and distributed around zero in the latter. Thus, RS cortex alone (in the range of cortical areas we were able to image) is responsible for leading the hippocampal gamma events, while ripple events are associated with a more spatially generalized flow of information from the hippocampus to the cortex (*SI Appendix*, Fig. S7).

Discussion

Quasi-Critical Nature of Cortical Spontaneous Activity during Sleep. We show here, with voltage imaging and ECoG, that neocortical spontaneous activity during sleep is largely made up by transient activations that follow the statistics of critical phenomena, most evident in natural sleep, where there is a tight fit with a power-law, signature of critical processes (Fig. 2*A* and *SI Appendix*, Fig. S2*A*).

In fact, computational models UP and DOWN states of non-rapid eye movement (NREM) cortical activity (47, 48) showed that recurrent excitation (which sustain UP states) and short-term synaptic depression (a candidate cause for UP state termination) are sufficient ingredients to obtain a (quasi)-critical distribution of UP state sizes.

We suggest that critical dynamics could play a very important role in systems memory consolidation processes. Any complex long-term memory will involve distributed traces at multiple, remote sites. The hippocampus is thought to generate rapidly constructed and readily retrievable index representations, which may ignite cortex-wide representations. Yet, this scheme poses the question of how the limited hippocampal input, propagated through relatively sparse long-range pathways may accomplish this feat. Critical dynamics is a regime of enhanced long-range correlations, yielding increased information storage (27) and transmission (49). As such, criticality facilitates the cortex-wide spread of hippocampal signals and provides a basis for coherent cortex-wide representations linking to the hippocampus. Indeed, coherent replay has been observed between the hippocampus and sensory areas with only an indirect, polysynaptic link with it, such as auditory (50) and visual cortex (10).

Cortical activity transients may also be self-ignited, reflecting spontaneous local processing and—during sleep—memory reactivation. Initial evidence that this may happen comes from magnetoencephalography studies with human subjects (51, 52) showing spontaneous replay events in the cortex. These cortex-originated transients may also provide a powerful input to the hippocampus, therefore participating in the two-way information exchange that we will discuss later.

Cortical Transients Activate Anatomically Defined Networks. Next, we show that multiscale activity transients are organized in cortex-wide networks. Our data-driven analysis demonstrates (Fig. 2 *C* and *D*), in a highly consistent fashion across two voltage imaging approaches, that small transient activations mostly remain confined to one of three networks, centered respectively on medial areas (with large overlap with the DMN) anterior sensorimotor cortices, and lateral cortex.

Enticingly, this tightly matches a network-theoretic analysis based on a massive amount of anatomical projection experiments. In the paper by Zingg et al. (28), a clustering of cortical connections is described in four networks. Our "RBM 2" (Fig. 2 *C* and *D*) component strongly overlaps with the "sensorimotor network" in that study, combining somatosensory and primary motor cortices. A set of "medial subnetworks" highlighted by Zingg et al. overlaps with our "RBM 3" component. That network, both in our data and in the anatomical characterization, is centered around the retrosplenial cortex and overlaps with the DMN as defined in the mouse brain (53). Our "RBM 1" component contains part of what Zingg et al. call the "posterior temporal lateral" network, which includes structures such as perirhinal and TeA cortices that are major players in the up and down streams of highly processed sensory information into the medial temporal lobe and eventually the hippocampus. An obvious limitation of our study is that, by imaging only dorsal cortices, we miss much of the lateral network in particular, as well as DMN areas, such as medial prefrontal cortex. Still, our data provide evidence that anatomical connectivity shapes the transient constituents of spontaneous activity, in a fashion that likely affects its function.

Larger transients eventually invade most of the recorded cortex and therefore cannot be allocated to specific clusters, but their origins follow the same topography. In fact, if we look at the cortical activity immediately preceding them, we see that the activity that ignites them is still circumscribed to one of the networks described above. Our "RBM 1" component (Fig. 2 *E–G*) shows activation confined to retrosplenial cortex and other areas in the DMN, whereas "RBM 2" shows transients with a sensorimotor origin.

The three functional networks that we identify in the mouse brain are rough equivalents of the more numerous resting-state networks found in the human brain (54) with fMRI. The time resolution of our voltage imaging enables us to closely follow the dynamics of these networks during sleep, to analyze, for example, how they may initiate whole-brain activity. Such generalized activations may potentially carry complex memories. The information reactivated by these networks may differ for the age or for the nature of the memory (e.g., implicit vs. explicit), which would have to be ascertained by further experiments.

Bidirectional Interactions between Cortical Networks and Hippocampal Activity. Our analysis of the link between cortical activation and hippocampal LFP points at a two-way interaction that involves multiple features of hippocampal activity. Our imaging data (Fig. 3) are consistent with the well-studied link between cortical activity and SWRs (4–7, 10, 13, 18, 55). Hippocampal ripple oscillation power correlates with small and

large transients (Fig. 3*B*) with similar intensity. Phase slope index (PSI), a pseudocausality analysis, suggests that ripple power predicts cortical transients (Fig. 4). Thus, SWRs and potentially replay are able to elicit widespread neocortical UP states at multiple spatial scales.

Yet, a surprisingly strong link was observed between hippocampal slow gamma and cortical transients. Whenever a comparison was possible, for example by partial correlation analysis, we found that the slow gamma link dominated the association between ripples and neocortical activity (Fig. 4*B* and *SI Appendix*, Fig. S6). PSI for slow gamma shows an opposite pseudocausality flow, from neocortical activity to hippocampal slow gamma. It is known that hippocampal activity is affected by cortical UP–DOWN state fluctuations (56, 57), even at the level of resting membrane potential (58). Here, we suggest that slow gamma oscillations are an important mediator of cortical influences.

The hippocampal physiology literature associates slow gamma with CA3 activity and possibly retrieval of information in that structure, which is widely seen as an auto-associative memory (31). During wakefulness, slow gamma oscillations fluctuate greatly (59). The instantaneous balance between slow gamma and medium gamma may reflect the momentary prevalence of respectively CA3 vs. entorhinal inputs into CA1 (29, 30). Correspondingly, a shift between memory retrieval, predictive hippocampal activity, and registration and storage of novel cortical inputs may take place (60) when slow gamma oscillations are larger. During sleep, SWR events associated to higher levels of slow gamma contain increased replay (32).

Our data may be explained by positing that cortical transients, by depolarizing neurons, may bias the hippocampal networks into a slow gamma–rich state. It is also likely in our view that the information content of the neocortical input will modulate which activity patterns will be retrieved (or generated) by the hippocampus. This interpretation is consistent with a bidirectional interaction between cortex and hippocampus (Fig. 5) during sleep. An enticing hypothesis, which would have to be explored experimentally and computationally, is that neocortex and hippocampus act in the sleep state as a single network, with transient activations that may be initiated in several points in the network and propagate at multiple scales, with e.g., the cortex biasing hippocampal activity (8, 57). This may enable neural plasticity continuous update of hippocampal representations as well as cortical representations, which may serve the function of keeping representations coherent across structures in face of substantial drift that has been observed across days (61, 62).

Thus, slow gamma and SWR are two signatures of retrieval processes in the hippocampus that are related but not completely overlapping. An interesting speculation is that while SWRs reflect "autonomous" hippocampal retrieval, slow gamma is strongest when retrieval takes place in a larger network, with hippocampal and neocortical components.

Retrosplenial Cortex and the DMN Preferentially Engage Hippocampal Activity. Importantly, not all neocortical activity transients interact with the hippocampus equally (18). The medial/DMN network is related to a significantly larger increase in slow gamma power in the hippocampus (Fig. 3 *A* and *B*) and with a tighter correlation (Fig. 3*C*) compared to the somatomotor network. Within the medial network, the role of retrosplenial cortex stands out: Not only is RS the hotspot for initiating large transients (RBM 1 in Fig. 2 *E* and *F*) but it is also the area whose activity most markedly predicts increases in hippocampal slow gamma. The rest of the medial network (and of the recorded neocortex) activates only following hippocampal activation (Fig. 4*E*). Thus, the medial/DMN network activation may activate independently of the hippocampus. In humans, the DMN has been found to activate in correspondence with replay bursts (63), suggesting that it plays a distinct role in memory retrieval and reactivation. Because the retrosplenial cortex, also a hub of the DMN, has been found to be a hub for remote memory reactivation (64), it is possible that the large transients initiating there do represent replay of older memories, to be interleaved with new memory replay, initiated by the hippocampus, a setup that is thought to be beneficial for memory consolidation. We speculate also that the RS-initiated replay may provide the semantic context for reprocessing in the hippocampus.

In summary, we presented a view of the global architecture of cortico-hippocampal interactions, which opens theoretical perspectives on the mechanisms of memory consolidation, in a view emphasizing two-way exchanges between these two brain areas key for memory and cognition.

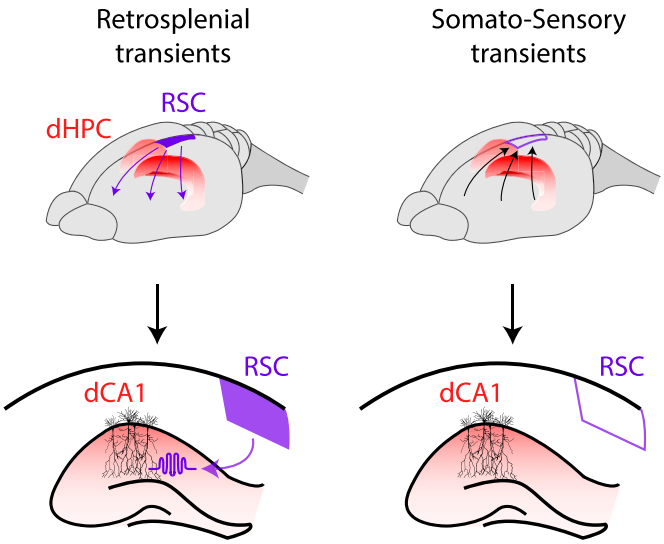

Fig. 5. Schematic of the hypothesized bidirectional interaction between the RS network and the hippocampus.

Materials and Methods

For detailed methods, see *SI Appendix*. All experiments were approved by the Animal Welfare Committee of the University of Lethbridge (urethane dataset) or by the Dutch Centraal Commissie Dierproeven and by the Radboud University Animal Welfare Board and conducted in accordance with the Experiments on Animals Act and the European Directive 2010/63/EU on animal research (sleep dataset). Imaging was carried out with wide-field cameras on the exposed brain surface (under urethane anesthesia; 1,250 mg/kg; voltage dye RH1691 from Optical Imaging) or through the thinned skull [sleep; Butterfly 1.2 Genetically Encoded Voltage indicator (33) expressed in transgenic line] at the appropriate wavelength for the fluorophores. Electrodes or linear silicon probes were implanted in the CA1 hippocampal subfield for LFP recording. For natural sleep recordings NREM and REM sleep periods were detected based on LFP features (theta/delta ratio), pupil size, and bodily movements. Current-source density analysis was performed on the linear probe traces to obtain layer-resolved hippocampal potentials.

Cortical transients were detected by a thresholding procedure and classified by training an RBM autoencoder on the pixel-by-pixel activation configurations and clustering the hidden layer weight configurations obtained. Pseudocausality analysis used the PSI measure (46) between the time series of the pixels in the imaging recording and of the bandpass-filtered hippocampal LFP.

Data, Materials, and Software Availability. The codes and electrophysiology and imaging data used in this work have been deposited in the Donders Repository [https://doi.org/10.34973/2w2s-tg07(65)].

ACKNOWLEDGMENTS. We acknowledge support from the European Commission Horizon 2020 program, grants ERC-AdG 833964 "REPLAY_DMN" (to F.P.B.), MSCA ITN 765549 "M-GATE" (to F.P.B.), MSCA Intraeuropean Fellowship 840704 "BrownianReactivation" (to F.S. and F.P.B.), and from Natural Sciences and Engineering Research Council of Canada (grants 40352 and 1631465 to M.H.M.), Alberta Innovates (to M.H.M.), Alberta Prion Research Institute (grant 43568 to M.H.M.), and Canadian Institute for Health Research (grants 390930 and 156040 to M.H.M.), NSF (to M.H.M.), and NIH (1U01NS099573 to T.K.). We thank J. Sun for surgical assistance, Matteo Guardamagna, Jeroen Bos, and Chenchen Song for technical advice, Tjitse van der Molen for help with data analysis, and Christophe Bernard and Loig Kergoat for donating the ECoG grids.

Author affiliations: [a]Donders Institute for Brain Cognition and Behaviour, Radboud University, 6525AJ Nijmegen, The Netherlands; [b]Canadian Centre for Behavioral Neuroscience, University of Lethbridge, Lethbridge, AB T1K 6 3M4, Canada; and [c]Laboratory for Neuronal Circuit Dynamics, Imperial College London, London SW7 2AZ, United Kingdom

1. J. R. Andrews-Hanna, The brain's default network and its adaptive role in internal mentation. *Neuroscientist* **18**, 251–270 (2012).
2. M. E. Raichle, The brain's default mode network. *Annu. Rev. Neurosci.* **38**, 433–447 (2015).
3. G. Buzsáki, Hippocampal sharp wave-ripple: A cognitive biomarker for episodic memory and planning. *Hippocampus* **25**, 1073–1188 (2015).
4. F. P. Battaglia, G. R. Sutherland, B. L. McNaughton, Hippocampal sharp wave bursts coincide with neocortical "up-state" transitions. *Learn. Mem.* **11**, 697–704 (2004).
5. N. K. Logothetis *et al.*, Hippocampal-cortical interaction during periods of subcortical silence. *Nature* **491**, 547–553 (2012).
6. A. Sirota, J. Csicsvari, D. Buhl, G. Buzsáki, Communication between neocortex and hippocampus during sleep in rodents. *Proc. Natl. Acad. Sci. U.S.A.* **100**, 2065–2069 (2003).
7. R. Kaplan *et al.*, Hippocampal sharp-wave ripples influence selective activation of the default mode network. *Curr. Biol.* **26**, 686–691 (2016).
8. F. P. Battaglia, K. Benchenane, A. Sirota, C. M. Pennartz, S. I. Wiener, The hippocampus: Hub of brain network communication for memory. *Trends Cogn. Sci.* **15**, 310–318 (2011).
9. J. O'Neill, B. Pleydell-Bouverie, D. Dupret, J. Csicsvari, Play it again: Reactivation of waking experience and memory. *Trends Neurosci.* **33**, 220–229 (2010).
10. D. Ji, M. A. Wilson, Coordinated memory replay in the visual cortex and hippocampus during sleep. *Nat. Neurosci.* **10**, 100–107 (2007).
11. N. Nitzan *et al.*, Propagation of hippocampal ripples to the neocortex by way of a subiculum-retrosplenial pathway. *Nat. Commun.* **11**, 1947 (2020).
12. H. F. Ólafsdóttir, F. Carpenter, C. Barry, Coordinated grid and place cell replay during rest. *Nat. Neurosci.* **19**, 792–794 (2016).
13. A. Peyrache, M. Khamassi, K. Benchenane, S. I. Wiener, F. P. Battaglia, Replay of rule-learning related neural patterns in the prefrontal cortex during sleep. *Nat. Neurosci.* **12**, 919–926 (2009).
14. T. J. Teyler, P. DiScenna, The hippocampal memory indexing theory. *Behav. Neurosci.* **100**, 147–154 (1986).
15. J. L. McClelland, B. L. McNaughton, R. C. O'Reilly, Why there are complementary learning systems in the hippocampus and neocortex: Insights from the successes and failures of connectionist models of learning and memory. *Psychol. Rev.* **102**, 419–457 (1995).
16. M. Moscovitch *et al.*, Functional neuroanatomy of remote episodic, semantic and spatial memory: A unified account based on multiple trace theory. *J. Anat.* **207**, 35–66 (2005).
17. M. J. Sekeres, M. Moscovitch, G. Winocur, "Mechanisms of memory consolidation and transformation" in *Cognitive Neuroscience of Memory Consolidation*, N. Axmacher, B. Rasch, Eds. (Studies in Neuroscience, Psychology and Behavioral Economics, Springer International Publishing, 2017), pp. 17–44.
18. J. Karimi Abadchi *et al.*, Spatiotemporal patterns of neocortical activity around hippocampal sharp-wave ripples. *eLife* **9**, e51972 (2020).
19. M. Steriade, A. Nuñez, F. Amzica, Intracellular analysis of relations between the slow (<1 Hz) neocortical oscillation and other sleep rhythms of the electroencephalogram. *J. Neurosci.* **13**, 3266–3283 (1993).
20. Y. Shu, A. Hasenstaub, A. Duque, Y. Yu, D. A. McCormick, Modulation of intracortical synaptic potentials by presynaptic somatic membrane potential. *Nature* **441**, 761–765 (2006).
21. M. Steriade, D. Contreras, R. Curró Dossi, A. Nuñez, The slow (< 1 Hz) oscillation in reticular thalamic and thalamocortical neurons: Scenario of sleep rhythm generation in interacting thalamic and neocortical networks. *J. Neurosci.* **13**, 3284–3299 (1993).
22. F. Amzica, M. Steriade, Short- and long-range neuronal synchronization of the slow (< 1 Hz) cortical oscillation. *J. Neurophysiol.* **73**, 20–38 (1995).
23. R. Huber, M. F. Ghilardi, M. Massimini, G. Tononi, Local sleep and learning. *Nature* **430**, 78–81 (2004).
24. M. H. Mohajerani, D. A. McVea, M. Fingas, T. H. Murphy, Mirrored bilateral slow-wave cortical activity within local circuits revealed by fast bihemispheric voltage-sensitive dye imaging in anesthetized and awake mice. *J. Neurosci.* **30**, 3745–3751 (2010).
25. M. H. Mohajerani *et al.*, Spontaneous cortical activity alternates between motifs defined by regional axonal projections. *Nat. Neurosci.* **16**, 1426–1435 (2013).
26. J. Wilting, V. Priesemann, Inferring collective dynamical states from widely unobserved systems. *Nat. Commun.* **9**, 2325 (2018).
27. J. Wilting, V. Priesemann, 25 years of criticality in neuroscience – Established results, open controversies, novel concepts. *Curr. Opin. Neurobiol.* **58**, 105–111 (2019).
28. B. Zingg *et al.*, Neural networks of the mouse neocortex. *Cell* **156**, 1096–1111 (2014).
29. A. Bragin *et al.*, Gamma (40-100 Hz) oscillation in the hippocampus of the behaving rat. *J. Neurosci.* **15**, 47–60 (1995).
30. L. L. Colgin *et al.*, Frequency of gamma oscillations routes flow of information in the hippocampus. *Nature* **462**, 353–357 (2009).
31. A. Treves, E. T. Rolls, Computational analysis of the role of the hippocampus in memory. *Hippocampus* **4**, 374–391 (1994).
32. M. F. Carr, M. P. Karlsson, L. M. Frank, Transient slow gamma synchrony underlies hippocampal memory replay. *Neuron* **75**, 700–713 (2012).
33. C. Song, D. M. Piscopo, C. M. Niell, T. Knöpfel, Cortical signatures of wakeful somatosensory processing. *Sci. Rep.* **8**, 11977 (2018).
34. D. Barson *et al.*, Simultaneous mesoscopic and two-photon imaging of neuronal activity in cortical circuits. *Nat. Methods* **17**, 107–113 (2020).
35. C. Ren, T. Komiyama, Wide-field calcium imaging of cortex-wide activity in awake, head-fixed mice. *STAR Protoc* **2**, 100973 (2021).
36. E. Bermudez-Contreras *et al.*, High-performance, inexpensive setup for simultaneous multisite recording of electrophysiological signals and mesoscale voltage imaging in the mouse cortex. *Neurophotonics* **5**, 025005 (2018).
37. W. Akemann, H. Mutoh, A. Perron, J. Rossier, T. Knöpfel, Imaging brain electric signals with genetically targeted voltage-sensitive fluorescent proteins. *Nat. Methods* **7**, 643–649 (2010).
38. W. Akemann *et al.*, Imaging neural circuit dynamics with a voltage-sensitive fluorescent protein. *J. Neurophysiol.* **108**, 2323–2337 (2012).
39. M. Carandini *et al.*, Imaging the awake visual cortex with a genetically encoded voltage indicator. *J. Neurosci.* **35**, 53–63 (2015).
40. G. Scott *et al.*, Voltage imaging of waking mouse cortex reveals emergence of critical neuronal dynamics. *J. Neurosci.* **34**, 16611–16620 (2014).
41. J. P. Neto, F. P. Spitzner, V. Priesemann, A unified picture of neuronal avalanches arises from the understanding of sampling effects. bioRxiv [Preprint] (2019). https://www.biorxiv.org/content/10.1101/759613v1. Accessed 1 March 2022.
42. U. Köster, J. Sohl-Dickstein, C. M. Gray, B. A. Olshausen, Modeling higher-order correlations within cortical microcolumns. *PLOS Comput. Biol.* **10**, e1003684 (2014).
43. A. Fernández-Ruiz *et al.*, Entorhinal-CA3 dual-input control of spike timing in the hippocampus by theta-gamma coupling. *Neuron* **93**, 1213–1226.e5 (2017).
44. V. Lopes-Dos-Santos *et al.*, Parsing hippocampal theta oscillations by nested spectral components during spatial exploration and memory-guided behavior. *Neuron* **100**, 940–952.e7 (2018).
45. A. N. Opalka, W. Q. Huang, J. Liu, H. Liang, D. V. Wang, Hippocampal ripple coordinates retrosplenial inhibitory neurons during slow-wave sleep. *Cell Rep.* **30**, 432–441.e3 (2020).
46. G. Nolte, A. Ziehe, N. Krämer, F. Popescu, K.-R. Müller, "Comparison of granger causality and phase slope index" in *Proceedings of Workshop on Causality: Objectives and Assessment at NIPS 2008* (PMLR, 2010), pp. 267–276.
47. A. Levina, J. M. Herrmann, T. Geisel, Dynamical synapses causing self-organized criticality in neural networks. *Nat. Phys.* **3**, 857–860 (2007).
48. D. Millman, S. Mihalas, A. Kirkwood, E. Niebur, Self-organized criticality occurs in non-conservative neuronal networks during up states. *Nat. Phys.* **6**, 801–805 (2010).
49. O. Shriki, D. Yellin, Optimal information representation and criticality in an adaptive sensory recurrent neuronal network. *PLOS Comput. Biol.* **12**, e1004698 (2016).
50. G. Rothschild, E. Eban, L. M. Frank, A cortical-hippocampal-cortical loop of information processing during memory consolidation. *Nat. Neurosci.* **20**, 251–259 (2017).
51. C. J. Higgins *et al.*, Replay bursts coincide with activation of the default mode and parietal alpha network. bioRxiv [Preprint] (2020). https://www.biorxiv.org/content/10.1101/2020.06.23.166645v1. Accessed 1 March 2022.
52. Y. Liu, R. J. Dolan, Z. Kurth-Nelson, T. E. Behrens, Human replay spontaneously reorganizes experience. *Cell* **178**, 640–652. e14 (2019).
53. J. M. Stafford *et al.*, Large-scale topology and the default mode network in the mouse connectome. *Proc. Natl. Acad. Sci. U.S.A.* **111**, 18745–18750 (2014).
54. J. S. Damoiseaux *et al.*, Consistent resting-state networks across healthy subjects. *Proc. Natl. Acad. Sci. U.S.A.* **103**, 13848–13853 (2006).
55. A. Peyrache, F. P. Battaglia, A. Destexhe, Inhibition recruitment in prefrontal cortex during sleep spindles and gating of hippocampal inputs. *Proc. Natl. Acad. Sci. U.S.A.* **108**, 17207–17212 (2011).
56. Y. Isomura *et al.*, Integration and segregation of activity in entorhinal-hippocampal subregions by neocortical slow oscillations. *Neuron* **52**, 871–882 (2006).
57. A. Sirota, G. Buzsáki, Interaction between neocortical and hippocampal networks via slow oscillations. *Thalamus Relat. Syst.* **3**, 245–259 (2005).
58. T. T. G. Hahn, B. Sakmann, M. R. Mehta, Phase-locking of hippocampal interneurons' membrane potential to neocortical up-down states. *Nat. Neurosci.* **9**, 1359–1361 (2006).
59. B. Lasztóczi, T. Klausberger, Hippocampal place cells couple to three different gamma oscillations during place field traversal. *Neuron* **91**, 34–40 (2016).
60. M. Guardamagna, F. Stella, F. P. Battaglia, Distinct hippocampal network states support theta phase precession and theta sequences in CA1. bioRxiv [Preprint] (2021). https://www.biorxiv.org/content/10.1101/2021.12.22.473863v1. Accessed 1 June 2022.
61. C. E. Schoonover, S. N. Ohashi, R. Axel, A. J. P. Fink, Representational drift in primary olfactory cortex. *Nature* **594**, 541–546 (2021).
62. Y. Ziv *et al.*, Long-term dynamics of CA1 hippocampal place codes. *Nat. Neurosci.* **16**, 264–266 (2013).
63. C. Higgins *et al.*, Replay bursts in humans coincide with activation of the default mode and parietal alpha networks. *Neuron* **109**, 882–893.e7 (2021).
64. K. K. Cowansage *et al.*, Direct reactivation of a coherent neocortical memory of context. *Neuron* **84**, 432–441 (2014).
65. R. Pedrosa. DCN data. Donders Database. https://doi.org/10.34973/2w2s-tg07. Accessed 1 September 2022.